MAJOR TECHNICAL ADVANCES

A Heterotopic Xenograft Model of Human Airways for Investigating Fibrosis in Asthma

Tillie-Louise Hackett[1], Sarah C. Ferrante[2], Claire E. Hoptay[3], John F. Engelhardt[4], Jennifer L. Ingram[5], Yulong Zhang[4], Sarah E. Alcala[3], Furquan Shaheen[1], Ethan Matz[2], Dinesh K. Pillai[2,6,7], and Robert J. Freishtat[2,7,8]

[1]Department of Anesthesiology, Pharmacology, and Therapeutics, Centre for Heart Lung Innovation, University of British Columbia, Vancouver, British Columbia, Canada; [2]Department of Integrative Systems Biology and [7]Department of Pediatrics, George Washington University School of Medicine and Health Sciences, Washington, D.C.; [3]Children's Research Institute: Center for Genetic Medicine Research, [6]Division of Pulmonary and Sleep Medicine, and [8]Division of Emergency Medicine, Children's National Health System, Washington, D.C.; [4]Department of Anatomy and Cell Biology, University of Iowa, Iowa City, Iowa; and [5]Division of Pulmonary, Allergy, and Critical Care Medicine, Duke University Health System, Durham, North Carolina

ORCID ID: 0000-0002-7411-2342 (R.J.F.).

Abstract

Limited *in vivo* models exist to investigate the lung airway epithelial role in repair, regeneration, and pathology of chronic lung diseases. Herein, we introduce a novel animal model in asthma—a xenograft system integrating a differentiating human asthmatic airway epithelium with an actively remodeling rodent mesenchyme in an immunocompromised murine host. Human asthmatic and nonasthmatic airway epithelial cells were seeded into decellularized rat tracheas. Tracheas were ligated to a sterile cassette and implanted subcutaneously in the flanks of nude mice. Grafts were harvested at 2, 4, or 6 weeks for tissue histology, fibrillar collagen, and transforming growth factor-β activation analysis. We compared immunostaining in these xenografts to human lungs. Grafted epithelial cells generated a differentiated epithelium containing basal, ciliated, and mucus-expressing cells. By 4 weeks postengraftment, asthmatic epithelia showed decreased numbers of ciliated cells and decreased E-cadherin expression compared with nonasthmatic grafts, similar to human lungs. Grafts seeded with asthmatic epithelial cells had three times more fibrillar collagen and induction of transforming growth factor-β isoforms at 6 weeks postengraftment compared with nonasthmatic grafts. Asthmatic epithelium alone is sufficient to drive aberrant mesenchymal remodeling with fibrillar collagen deposition in asthmatic xenografts. Moreover, this xenograft system represents an advance over current asthma models in that it permits direct assessment of the epithelial–mesenchymal trophic unit.

Keywords: asthma; remodeling; lung

Clinical Relevance

We developed a human asthmatic airway epithelial xenograft system as an animal model in asthma and demonstrate that the asthmatic airway epithelium alone can drive airway remodeling. This xenograft model is an advance over current animal models for asthma in that it permits direct assessment of the epithelial–mesenchymal trophic unit.

(Received in original form February 17, 2016; accepted in final form October 11, 2016)

This work was supported by National Institutes of Health National Center for Advancing Translational Sciences award UL1TR000075. Additional funding support was provided by the Clark Charitable Foundation (Bethesda, MD).

The contents of this article are solely the responsibility of the authors and do not necessarily represent the official views of the National Center for Advancing Translational Sciences or the National Institutes of Health.

Author Contributions: T.L.-H., S.C.F., C.E.H., J.L.I., Y.Z., S.E.A., F.S., E.M., and R.J.F. performed the experiments; T.L.-H., S.C.F., C.E.H., and R.J.F. analyzed the data; T.L.-H., J.F.E., J.L.I., D.K.P., and R.J.F. contributed reagents/materials/analysis tools; T.L.-H., S.C.F., C.E.H., J.F.E., D.K.P., and R.J.F. contributed to writing the manuscript.

Correspondence and requests for reprints should be addressed to Robert J. Freishtat, M.D., M.P.H., Division of Emergency Medicine, Children's National Health System, 111 Michigan Avenue, Northwest, Washington, D.C. 20010. E-mail: rfreishtat@childrensnational.org

This article has an online supplement, which is accessible from this issue's table of contents at www.atsjournals.org

Am J Respir Cell Mol Biol Vol 56, Iss 3, pp 291–299, Mar 2017

Originally Published in Press as DOI: 10.1165/rcmb.2016-0065MA on October 27, 2016
Internet address: www.atsjournals.org

The airway epithelium forms the interface between the external environment and the lung parenchyma. In addition to its barrier function, the airway epithelium plays an important role in the maintenance of lung homeostasis (1) by interacting with the innate and adaptive immune systems (2) and through cross-talk with the underlying mesenchyme (3, 4). Due to the complexity of the airway, which consists of multiple interacting cell types, the development of an adequate human model to understand the role of the airway epithelium in both lung homeostasis and the pathology of chronic lung disease has proven difficult. Furthermore, the contributions of specific cells and tissues (epithelial, immune, and connective) to aberrant remodeling and fibrosis in chronic lung diseases have been difficult to define.

In acting as a barrier, the airway epithelium is exposed to pathogens and toxins, leading to repeated cycles of injury and repair. These repair processes are defective in asthma, as evidenced by a reduction in the cell–cell adhesion proteins involved in barrier function (5), asynchrony in mitotic cell division, and increased production of inflammatory mediators and growth factors, such as transforming growth factor (TGF)-β1 (6–9).

To date, studies of diseased airway cells and tissues have largely been limited to *in vitro* data (10, 11). *In vivo* allergic animal models of asthma, such as those using ovalbumin sensitization, support a causative relationship between abnormal epithelial regenerative processes and fibrosis (8, 9). However, these animal models for asthma involve immune activation and obscure direct examination of the epithelial–mesenchymal trophic unit, critical for asthmatic airway remodeling (1). The direct study of the epithelial–mesenchymal trophic unit and its role in asthmatic airway remodeling requires an *in vivo* airway system consisting of three elements: human diseased airway epithelium, reactive mesenchyme, and absence of a functional immune system. Although attempts have been made to humanize animal lungs (12), no current asthma model meets all three requirements. The inadequacy of animal models for asthma and other respiratory diseases is a major factor in the failure of promising drug candidates to translate from animals to humans (13). As such, the cumulative probability of a new respiratory drug reaching the marketplace is less than half that for drugs targeting diseases in other organ systems (13).

This study demonstrates the development of a novel xenograft system that allows for assessing the properties of asthmatic airway epithelium without confounding effects of immune regulation, and that has potential to be similarly used to assess the properties of epithelia from patients with other pulmonary diseases, and to assess the efficacy of experimental therapies. Using this model, we show that asthmatic epithelium alone is sufficient to drive aberrant mesenchymal remodeling. Furthermore, this model provides a novel system to study drug targets for asthmatic lung function decline, for which there are no current therapies (14).

Materials and Methods

Antibody details are available in the supplementary Materials and Methods.

Ethics Statement

All animal studies were performed in strict accordance with the recommendations of the National Institutes of Health under Children's National Health System Institutional Animal Care and Use Committee Protocol 00030394. All surgery was performed under isoflurane anesthesia.

Cells and Tissues

Human primary airway epithelial cells from donors with and without asthma were obtained commercially from Lonza, Inc. (Walkersville, MD). Rat tracheas were harvested from male 200- to 250-g Fisher 344 rats (Charles River Laboratories, Inc., Wilmington, MA) and decellularized via three freeze–thaw cycles. Nontransplantable human lungs from donors with asthma and those without were donated for research through the International Institute for the Advancement of Medicine (Edison, NJ).

Xenografts

Assembled xenograft cassettes were seeded with 2×10^6 human airway epithelial cells, as previously described (15), and then implanted subcutaneously in the flanks of male 20- to 25-g Nu/Nu athymic mice (The Jackson Laboratory, Bar Harbor, MA). Acellular control xenografts were seeded with media only. Xenografts were flushed weekly with 1 ml of prewarmed (37°C) Ham's F12 (Lonza, Inc.) followed by 2 ml of room air. Xenografts were harvested at 2, 4, and 6 weeks after seeding and split for storage as either flash-frozen or formalin-fixed and paraffin-embedded tissue.

Immunohistochemistry

Immunohistochemistry was performed on graft sections using an anti–E-cadherin monoclonal antibody, Alcian blue, or hematoxylin. Five images per section were captured by phase-contrast digital microscopy (Spot Imaging Solutions, Sterling Heights, MI) and two sections from each xenograft were analyzed ($n = 5$ xenografts per group) by a blinded observer for percent positive staining per unit length of basement membrane using Image-Pro Plus (Media Cybernetics, Rockville, MD). In Alcian blue-stained sections, ciliated and mucus positive cells were determined by point counting using Image-Pro Plus.

Immunofluorescence

Immunofluorescent staining was performed using anti–TGF-β1, anti–Smad3, anti–TGF-β2, anti–epidermal growth factor (EGF), or anti–α-smooth muscle actin (α-SMA) antibodies. Nuclei were counterstained with 4′,6-diamidino-2-phenylindole and slides were mounted with Prolong Gold Anti-fade reagent (Life Technologies, Carlsbad, CA). We used Image J software (https://imagej.nih.gov/ij/index.html) to determine average pixel count for each fluorescent channel and then calculated a positive:negative pixel expression ratio in the visualized area of tissue.

Second Harmonic Generation Microscopy

Flash-frozen or formalin-fixed and paraffin-embedded sections were counterstained with hematoxylin for visualization and imaged using second harmonic generation (SHG) microscopy to determine fibrillar collagen. Two sections per xenograft were cut, five images per section were captured ($n = 5$ xenografts per group), and images were analyzed by a blinded observer. Image analysis was performed using Volocity software (Improvisions, Inc., Coventry, UK).

Statistical Analyses

Statistical tests were performed in SPSS 23 software (IBM Corp., Armonk, NY) using two-tailed *t* test functions of log-transformed data within time points. Results are reported as mean (±SD) unless otherwise noted. Significance level was *P* less than or equal to 0.05.

Results

Establishment of the Asthmatic Airway Epithelial Xenograft System

We adapted a cystic fibrosis airway epithelial xenograft model to asthma (15). Briefly, primary human airway epithelial cells from five donors with asthma and five without asthma (Table 1, no significant differences between groups) were seeded in subcutaneously implanted decellularized rat tracheas, which were ligated to plastic cassettes that enable exposure to ambient air (Figure 1A). For each time point, primary epithelial cells from all 10 donors were used for xenograft seeding. In addition, five decellularized rat tracheas were grafted without cells as acellular controls.

Because the xenografts are comprised of three species (i.e., *Homo sapiens*, *Rattus rattus*, *Mus musculus*), we had the ability to locate each species in the xenografts.

Table 1. Demographics of Lung Airway Epithelial Cell Donors

Age (*Yr*)	Sex	Smoking	Medication
Subjects with asthma			
19	F	None	Unknown
25	M	None	Albuterol
52	F	None	Albuterol, fluticasone, salmeterol
52	M	None	Albuterol, fluticasone, prednisone, salmeterol
57	M	None	Albuterol, prednisone
Mean ± SD, 41 ± 18	3 M:2 F		
Subjects without asthma			
13	M	None	None
17	F	None	None
47	M	None	None
54	M	None	None
68	M	None	None
Mean ± SD, 40 ± 24	4 M: 1 F		
P = 0.93	*P* = 0.49	N/A	N/A

Definition of abbreviation: N/A, not applicable.

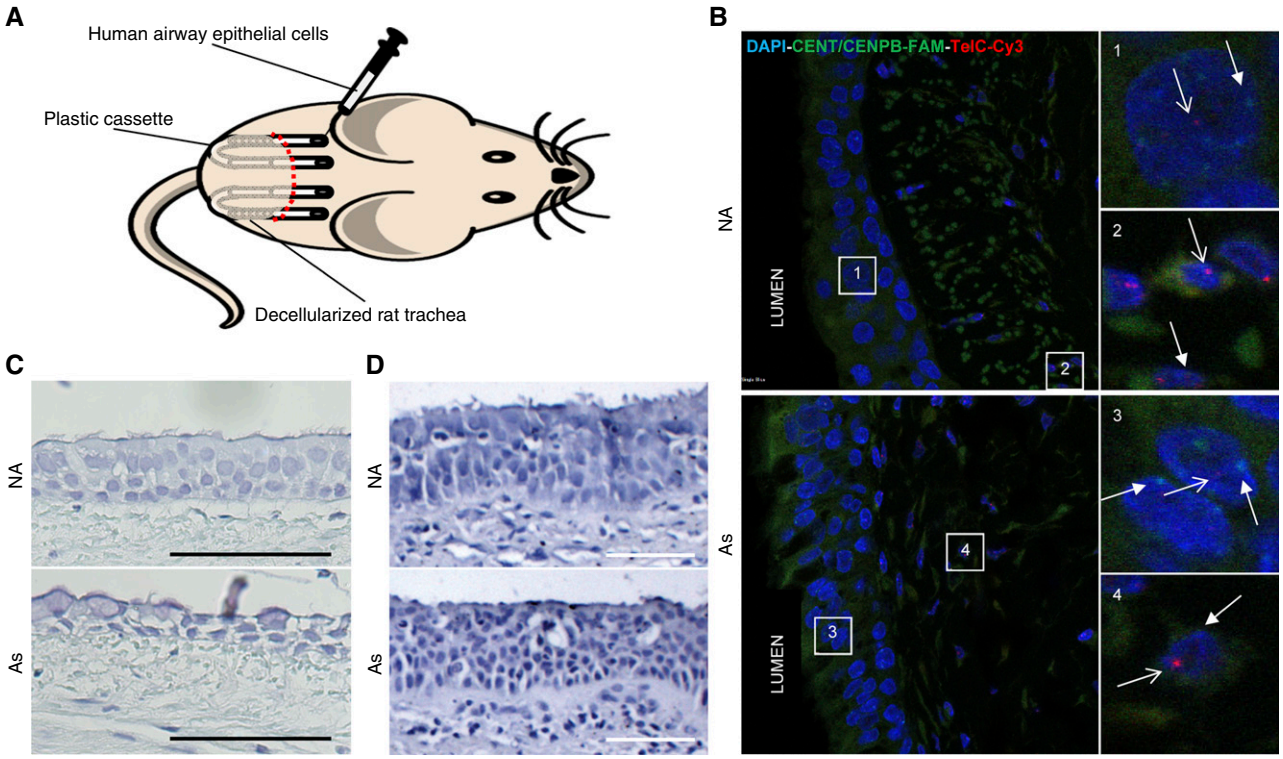

Figure 1. Epithelial morphology is similar in human airway tissue and xenografts. (*A*) Xenograft schematic. (*B*) *In situ* hybridization for pancentromere (human- and murine-specific sequences; *green*) and telomere (*red*) peptide nucleic acid probes in nonasthmatic (NA; *top panel*) and asthmatic (As; *bottom panel*) xenografts at 6 weeks postengraftment. *Green* and *dim red* nuclear staining (*insets 1* and *3*) denote cells of human origin, comprising the epithelium. *Green* and *bright red* nuclear staining (*insets 2* and *4*) denote cells of murine origin within the xenograft matrix. *Arrows* mark *green* and *red* staining for improved visibility. (*C*) Nonasthmatic (*top panel*) and asthmatic (*bottom panel*) airway epithelial xenografts at 6 weeks postengraftment stained for hematoxylin. (*D*) Representative hematoxylin staining of airway epithelium from nonasthmatic (*top panel*) and asthmatic (*bottom panel*) human airway tissue. *Scale bars*, 100 μm. CENPB, human centromere protein B; CENT, human α satellite centromere; DAPI, 4′,6-diamidino-2-phenylindole; TelC, C-rich telomere.

To accomplish this, we took advantage of interspecies telomeric and centromeric differences and performed fluorescent *in situ* hybridization (FISH) on xenografts at 6 weeks. Telomeres in commonly used inbred laboratory rodent strains are longer than human telomeres (50–150 kb in rodents versus 5–10 kb in humans). This difference in length results in a difference in the intensity of telomeric FISH signals (16, 17). Thus, we used peptide nucleic acid probes specific for mammalian telomeres in combination with probes for human and murine (not rat) centromeres to determine speciation of xenograft cells (17). Cells of human origin were characterized by a positive FISH signal for the centromeric probe and dim fluorescent intensity for the telomeric probe. Cells of murine origin were characterized by both a positive FISH signal for the centromeric probe and bright fluorescent intensity for the telomeric probe. Rat cells, which would have had bright fluorescence for the telomeric probe only, were not found in the decellularized rat tracheal tissue, as expected. For both nonasthmatic and asthmatic xenografts, we confirmed that cells located at the luminal surface and attached to the basement membrane, the normal location for airway epithelium, were uniformly of human origin, whereas cells occupying the mesenchyme were uniformly of murine origin (Figure 1B).

Next, we assessed the morphology of the xenograft system to determine resemblance to human lungs. Nonasthmatic epithelium that had been seeded in the xenograft model for 6 weeks generated a pseudostratified airway epithelium complete with ciliated, goblet, and basal cells (Figure 1C), comparable to normal human bronchial epithelium (Figure 1D). Asthmatic epithelium, on the other hand, did not develop a pseudostratified epithelium by 6 weeks postengraftment. This altered epithelial morphology bears a resemblance to human asthmatic bronchial tissue. However, the goblet cell hyperplasia typical in asthmatic bronchi (Figure 2A) was not replicated in the asthmatic xenografts at 6 weeks postengraftment (Figure 2B).

An important feature of asthma is the loss of junction proteins in the airway epithelium (18), such as E-cadherin (19). This is demonstrated in asthmatic human airway tissue by a 35% lower level of E-cadherin compared with nonasthmatic tissues (Figure 2C). Similarly, there was a significant decrease in E-cadherin staining in asthmatic compared with nonasthmatic xenografts at 4 weeks (mean ± SD: 26 ± 26% versus 50 ± 20%, $P = 0.003$) and 6 weeks (37 ± 31% versus 58 ± 16%, $P = 0.007$) postengraftment ($n = 5$ per group) (Figure 2D).

Evaluation of Airway Remodeling in the Asthmatic Xenograft

Our xenograft system allows for the study of disease-derived airway epithelium and its role in airway fibrosis. Therefore, we sought to determine if asthmatic epithelium alone is sufficient to drive aberrant

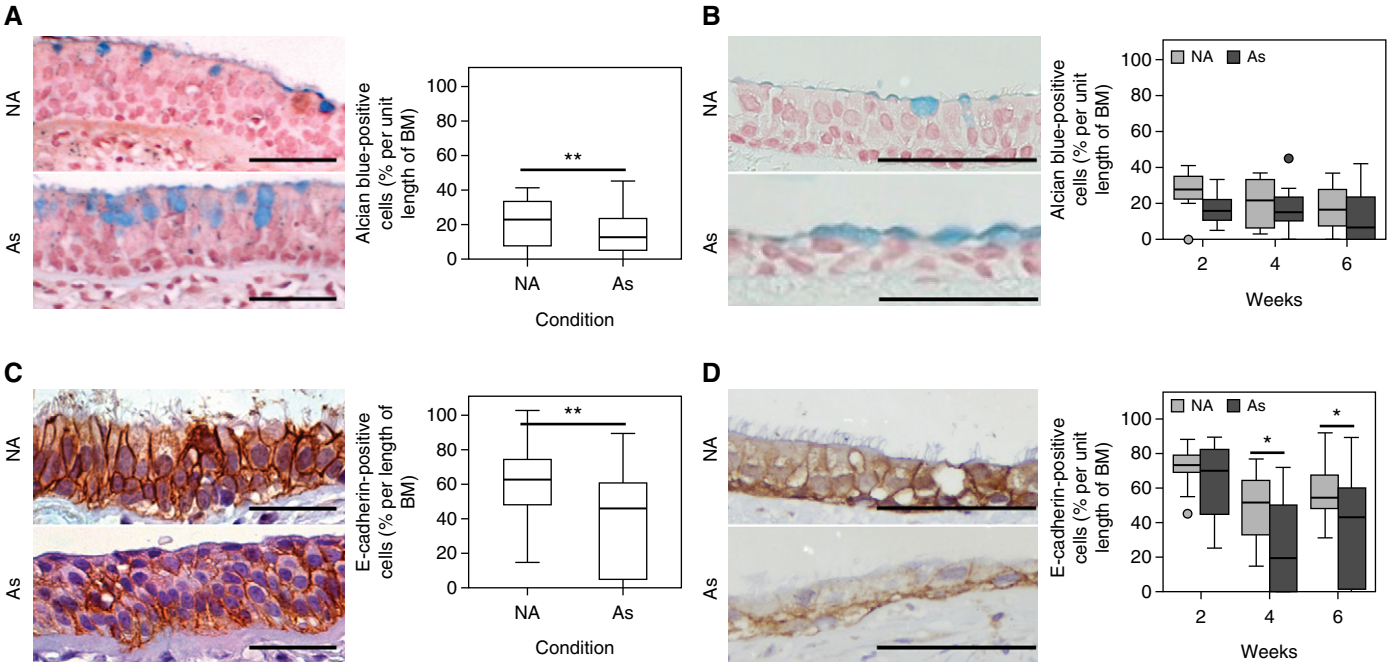

Figure 2. Asthmatic xenografts reflect mucus and E-cadherin expression in asthmatic human airway tissue. (*A*) Representative Alcian blue staining (i.e., mucus positive) of nonasthmatic (NA; *top panel*) and asthmatic (As; *bottom panel*) human airway tissue are shown. Alcian blue–positive epithelial cells are increased in asthmatic compared with nonasthmatic tissues (*right panel*). (*B*) Representative Alcian blue staining at 6 weeks postengraftment for nonasthmatic (*top panel*) and asthmatic (*bottom panel*) xenografts. Quantification of Alcian blue–positive epithelial cells at 2, 4, and 6 weeks postengraftment show no significant differences (*right panel*). (*C*) Representative E-cadherin staining in nonasthmatic (*top panel*) and asthmatic (*bottom panel*) human airway tissue. Asthmatic tissues show decreased E-cadherin staining compared with nonasthmatic controls (*right panel*). (*D*) Representative E-cadherin staining at 6 weeks postengraftment for nonasthmatic (*top panel*) and asthmatic (*bottom panel*) xenografts. Quantification of E-cadherin–positive epithelial cells (*right panel*) shows decreased staining in asthmatic compared with nonasthmatic xenografts at 4 and 6 weeks postengraftment. *Scale bars*, 100 μm. *Boxplots* represent medians (*thick line*), interquartile range (*box*), and 95% confidence interval (*error bars*). *Circles* denote outliers. $^{*}P \leq 0.05$, $^{**}P \leq 0.01$; $n = 5$ per group. BM, basement membrane.

mesenchymal remodeling, as measured by collagen deposition. Both human asthmatic bronchial tissue (Figure 3A) and asthmatic xenografts demonstrated increased collagen deposition in the basement membrane and subepithelium in comparison to nonasthmatic samples (Figure 3B).

As Masson's trichrome cannot differentiate between collagen types, we used SHG multiphoton microscopy to measure fibrillar collagens I and III, characteristic of scar tissue. The SHG signal for fibrillar collagen I and III is significantly elevated in asthmatic compared with nonasthmatic xenografts at 2 weeks (33 ± 15% versus 12 ± 4%, $P = 0.03$) and 6 weeks (28 ± 15% versus 9 ± 3%, $P = 0.04$) postengraftment ($n = 5$ per group; Figures 3C and 3D). In addition, staining for the mesenchymal marker, α-SMA, revealed clusters of SMA-positive murine cells located in the mesenchyme of asthmatic, but not nonasthmatic, xenografts (Figure 3E).

TGF-β1 and Xenograft Remodeling

Fibrogenic communication within the epithelial–mesenchymal trophic unit is mediated by growth factors, particularly TGF-β1, which are elevated in the airways of patients with asthma (20). Given the presence of fibrosis and α-SMA–positive mesenchymal cells in the asthmatic xenografts, we assayed the xenografts for TGF-β1 and phosphorylated (p) Smad3, a transcriptional modulator activated in canonical TGF-β1 signaling (21). Mesenchymal cells in asthmatic xenografts showed significantly higher TGF-β1 expression ratios (i.e., positive:negative pixels) than in nonasthmatics xenografts at 4 weeks (0.12 ± 0.01 versus 0.05 ± 0.01, $P = 0.003$) and 6 weeks (0.09 ± 0.02 versus 0.04 ± 0.02, $P = 0.04$) postengraftment ($n = 5$ per group; Figure 4). Concordantly, asthmatic grafts showed significantly higher expression of pSmad3 than nonasthmatic controls at 4 weeks (0.11 ± 0.04 versus 0.06 ± 0.02, $P = 0.04$) and 6 weeks (0.08 ± 0.01 versus 0.03 ± 0.02, $P = 0.02$) postengraftment ($n = 5$ per group; Figure 4).

TGF-β2 and EGF in Xenograft Remodeling

To provide additional evidence for fibrogenic communication within the xenograft epithelial–mesenchymal trophic unit, we examined the expression of TGF-β2 and EGF. TGF-β2 is the predominant isoform expressed in severe asthma, and is

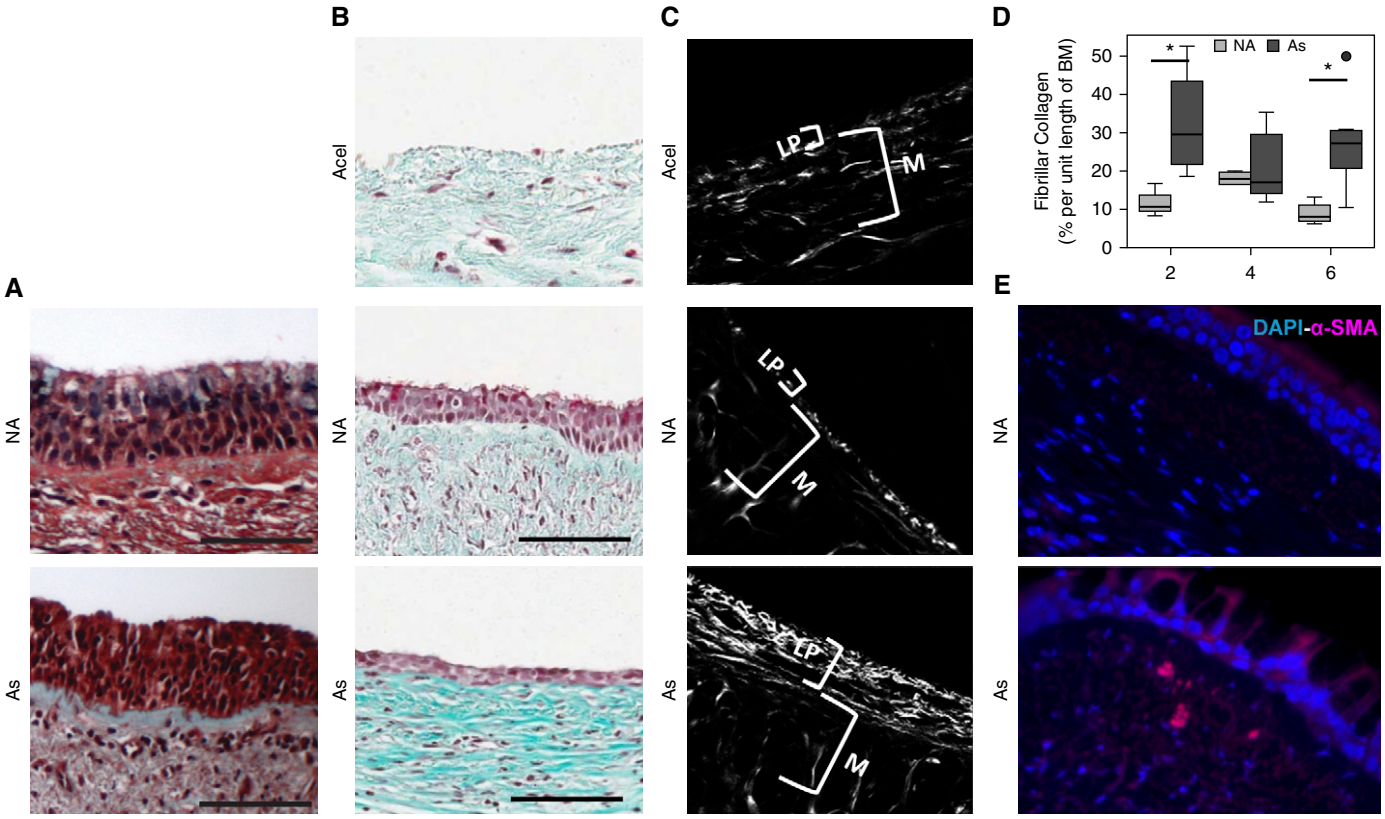

Figure 3. Matrix remodeling during epithelial regeneration differs between asthmatic and nonasthmatic epithelia. (*A*) Masson's trichrome staining of nonasthmatic (NA; *top panel*) and asthmatic (As; *bottom panel*) human airway tissues demonstrates increased staining of collagen (*blue/green*) in the basement membrane and subepithelium of asthmatic compared with nonasthmatic tissue. (*B*) Xenograft sections from 6-week postengraftment stained with Masson's trichrome demonstrate abundant collagen accumulation in asthmatic (*bottom panel*) compared with nonasthmatic (*middle panel*) xenografts. An acellular (Acel; *top panel*) xenograft is shown for comparison. (*C*) Images from second harmonic generation (SHG) microscopy demonstrate the SHG signal specific to fibrillar collagen (*gray*) in a nonasthmatic xenograft shown in the *middle panel*, and asthmatic xenograft, as shown in the *bottom panel*. An acellular (*top panel*) xenograft is shown for comparison. LP, lamina propria; M, matrix. (*D*) Analyses of SHG signals demonstrate fibrillar collagen is elevated in asthmatic compared with nonasthmatic xenografts at 2 and 6 weeks postengraftment. (*E*) Fluorescent images of xenografts at 6 weeks showing clusters of α-smooth muscle actin (α-SMA; *red*) amid total cell nuclei (DAPI; *blue*) in asthmatic (*bottom panel*) but not nonasthmatic (*top panel*) grafts. *Scale bars*, 100 μm. *Boxplots* represent medians (*thick line*), interquartile range (*box*), and 95% confidence interval (*error bars*). *Circle* denotes outliers. $^*P \leq 0.05$; $n = 5$ per group.

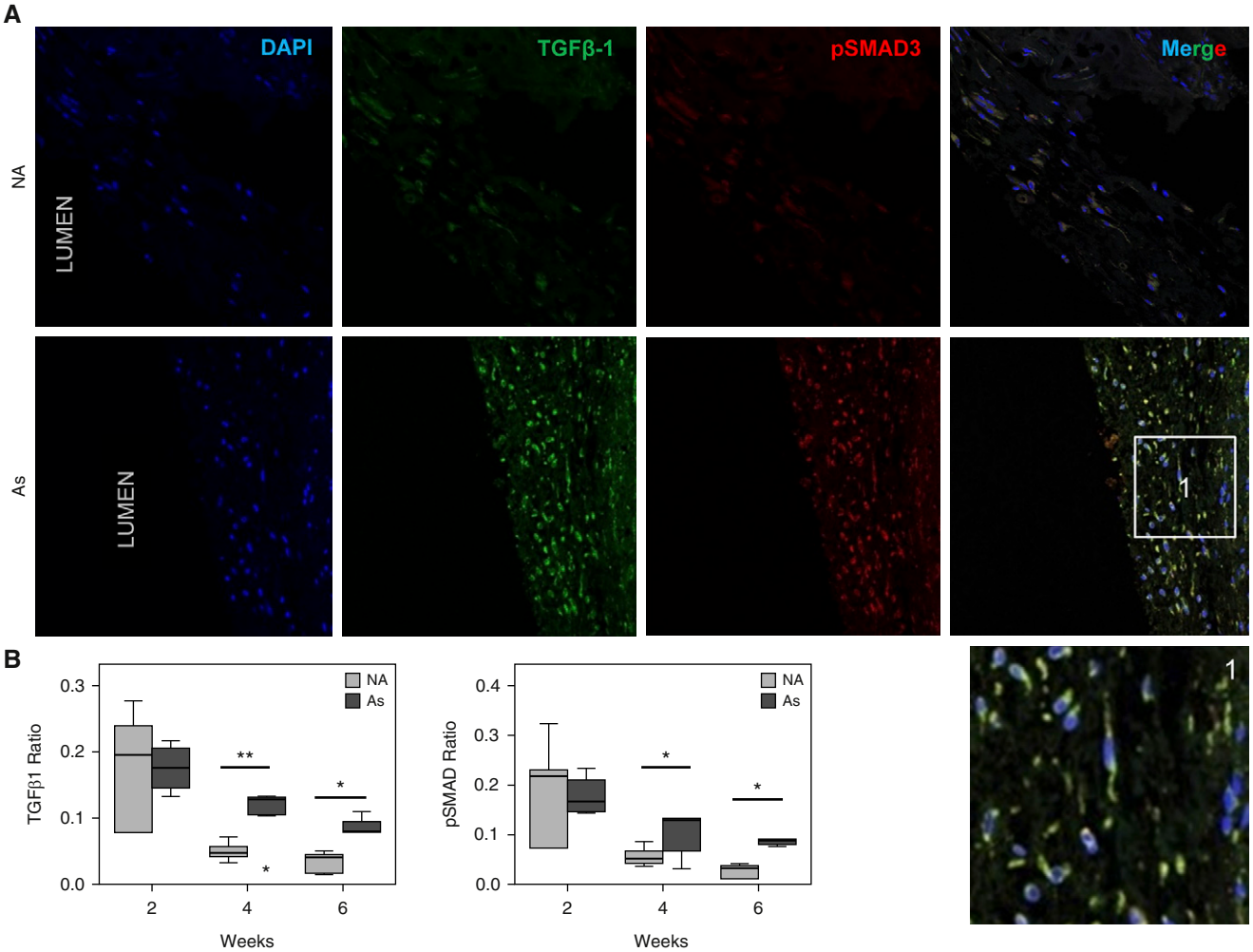

Figure 4. Transforming growth factor (TGF)-β1 signaling is elevated in asthmatic xenografts. (*A*) Confocal images of xenografts at 4 weeks show increased expression of both TGF-β1 (*green*) and pSMAD3 (*red*) in asthmatic (*bottom panels*) versus nonasthmatic (*top panels*) xenografts. An expanded image of mesenchymal cells merged for both TGF-β1– and pSMAD3-positive (*yellow*) cells is shown (*inset 1*). (*B*) Asthmatic (As) grafts show significantly increased ratios (positive: negative pixels) of TGF-β1 (*left panel*) and pSMAD3 (*right panel*) compared with nonasthmatic (NA) xenografts at 4 and 6 weeks postengraftment. *Boxplots* represent medians (*thick line*), interquartile range (*box*), and 95% confidence interval (*error bars*). $^{*}P \leq 0.05$, $^{**}P \leq 0.01$; $n = 5$ per group. pSMAD, phosphorylated SMAD.

associated with airway fibrosis (22), whereas EGF is a key contributor to airway remodeling and airway smooth muscle proliferation in asthma (23, 24). We found significantly higher TGF-β2 expression ratios (i.e., positive:negative pixels) in mesenchymal cells from asthmatic xenografts compared with cells from nonasthmatic xenografts at 2 weeks (0.13 ± 0.06 versus 0.04 ± 0.03, $P = 0.03$) and 4 weeks (0.21 ± 0.07 versus 0.04 ± 0.03, $P = 0.002$) postengraftment ($n = 5$ per group; Figure 5). In addition, asthmatic grafts showed significantly higher expression of EGF than nonasthmatic controls at 4 weeks postengraftment (0.18 ± 0.06 versus 0.07 ± 0.03, $P = 0.008$, $n = 5$ per group; Figure 5).

Discussion

Herein, we introduce a novel xenograft system that allows for assessing the properties of asthmatic airway epithelium without confounding effects of immune regulation, and that has potential to be similarly used to assess the properties of epithelia from patients with other pulmonary diseases and to assess the efficacy of experimental therapies. By combining a diseased airway epithelium and reactive mesenchyme in the absence of a functional immune system in an *in vivo* airway system, these xenografts permit direct assessment of the epithelial–mesenchymal trophic unit and are an advance over current animal models of asthma. Indeed, our work with this model provides the first *in vivo* evidence that asthmatic epithelium alone is sufficient to drive aberrant airway remodeling.

As with other airway xenograft systems (15, 25), our model replicates important aspects of human asthmatic and nonasthmatic lung biopsy tissue. Specifically, xenografted primary epithelial cells generate a differentiated epithelium containing basal, ciliated, and mucus-expressing cells. Nonasthmatic xenografted cells differentiate into an organized, pseudostratified epithelium, similar to human bronchial tissue from donors without asthma. In contrast, asthmatic grafted cells formed a nonuniform, poorly

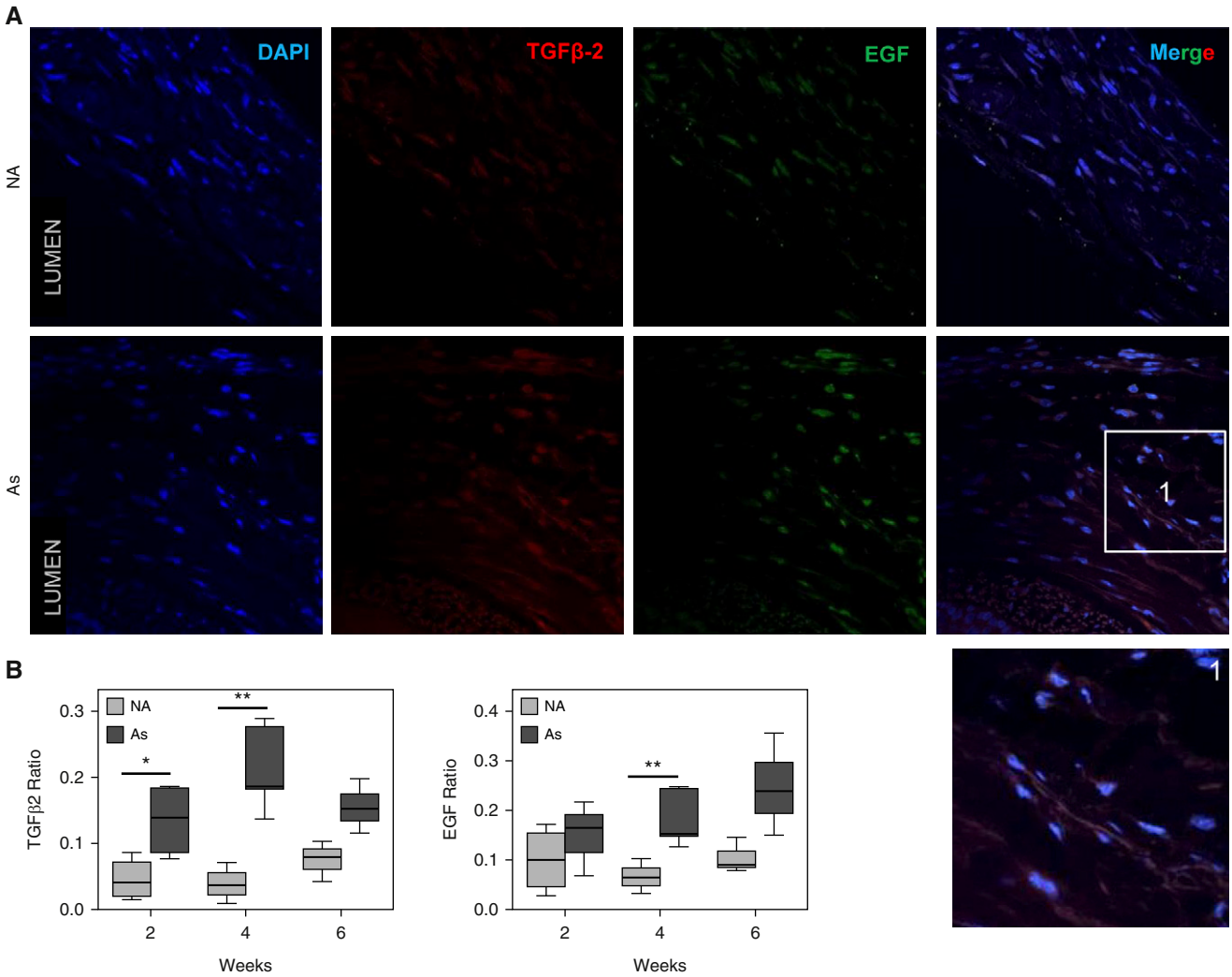

Figure 5. TGF-β2 and epidermal growth factor (EGF) signaling are elevated in asthmatic xenografts. (*A*) Confocal images of xenografts at 4 weeks show increased expression of both TGF-β2 (*red*) and EGF (*green*) in asthmatic (As; *bottom panels*) versus nonasthmatic (NA; *top panels*) xenografts. An expanded image of mesenchymal cells merged for both TGF-β2– and EGF-positive cells is shown (*inset 1*). (*B*) Asthmatic grafts show significantly increased ratios (positive:negative pixels) of TGF-β2 (*left panel*) and EGF (*right panel*) compared with nonasthmatic xenografts at 2 and/or 4 weeks postengraftment. *Boxplots* represent medians (*thick line*), interquartile range (*box*), and 95% confidence interval (*error bars*). $^{*}P \leqslant 0.05$, $^{**}P \leqslant 0.01$; $n = 5$ per group.

organized epithelium, reminiscent of human lung biopsies from donors with asthma. Furthermore, as the airway epithelium is the structural barrier to the external environment for the lung (26), loss of expression of the adhesion molecule, E-cadherin, indicates a dysfunctional barrier (27). Both the asthmatic grafted epithelium and the asthmatic human lung biopsy tissue show decreased E-cadherin expression. This is all consistent with our previous work showing that, when differentiated at air–liquid interface culture, asthmatic-derived epithelial cells are less differentiated in comparison to nonasthmatic-derived cells, as demonstrated by increased basal cell number and lack of E-cadherin (5, 6, 11, 19).

Although the xenografts are largely similar to human lung biopsies, there is a notable difference. Asthmatic xenografted epithelia showed mucus hypersecretion similar to asthmatic bronchi; however, there was no evidence of goblet cell hyperplasia in the xenografts. In experiments using air–liquid interface epithelial cultures, goblet cell hyperplasia is not an intrinsic feature of the asthmatic epithelium. Goblet cell hyperplasia occurs only when these cultures are exposed to Th2 cytokines, such as IL-13 (28, 29). Thus, it is possible that the absence of a functional Th2 response in our model prevents xenograft goblet cell hyperplasia.

Asthmatic airway remodeling is characterized by airway epithelial goblet cell hyperplasia and damage, airway smooth muscle hypertrophy, neovascularization, deposition of interstitial collagens, and thickening of the lamina reticularis (30–32). This remodeling is due to persistent activation of the epithelial–mesenchymal trophic unit and secretion of extracellular matrix proteins and TGF-β1 (10, 26). We interrogated our model for select characteristics of remodeling, including collagen deposition and growth factor secretion.

First, we demonstrate using SHG microscopy that asthmatic airway epithelium alone can drive subepithelial fibrillar collagen deposition, reminiscent of asthmatic airway remodeling. SHG microscopy is a multiphoton technique that provides direct information on the molecular ordering of microscopic structures. It was first shown in 1978 that fibrillar collagens, consisting of three parallel, intertwined, polar helices, are noncentrosymmetric structures that can be imaged using SHG microscopy (33). This is commonly achieved by detecting second-harmonic signals from the peptidic bonds of the triple helix of α-collagen (34). Nonfibrillar collagens, such as collagen IV, do not have a triple helix structure. As such, they do not emit a second-harmonic signal and cannot be imaged using this technique. For the past 10 years, SHG microscopy has commonly been used to image fibrillar collagen in multiple biological tissues, including heart, skin, eye, and lung (35).

The primary cells responsible for fibrillar and nonfibrillar collagen secretion within the body are mesenchymal cells, specifically fibroblasts. Upon migration to a wound site, fibroblasts undergo a phenotypic transformation to myofibroblasts (36, 37) and transition their major function to protein synthesis and production of extracellular matrix proteins, including fibronectin and collagen. Deposition of fibrillar collagens I and III, like that seen in our model, enables remodeling and contraction of the wound via these actin-rich myofibroblasts (37, 38).

Growth factors, such as TGF-β1, play an important role in stimulating fibroblasts to both migrate (39, 40) and differentiate into collagen-secreting myofibroblasts (20). We and others (6, 11, 41) have shown previously that basolateral secretion of TGF-β1 is increased from asthmatic airway epithelium *in vitro*. The current study furthers that work by demonstrating increased TGF-β1 in asthmatic xenografts, an *in vivo* system. Given the cross-reactivity between human TGF-β1 and the murine TGF-β1 receptor (42, 43), release of TGF-β1 by the human asthmatic airway epithelium in the xenografts may be responsible for inducing migration of murine α-SMA–positive mesenchymal cells into the subepithelium. Our finding of increased canonical TGF-β1 signaling in the mesenchymal cells present within the subepithelial tissue supports this.

We also demonstrate increased TGF-β2 in asthmatic xenografts, an important TGF-β isoform predominantly expressed in severe asthma (22). TGF-β2 has been implicated in profibrotic responses in the underlying mesenchyme (22), and is able to induce the differentiation of fibroblasts into myofibroblasts (44).

In addition, we found increased EGF in asthmatic xenografts. EGF is up-regulated in asthmatic human airways (23, 45) and is essential for epithelial repair (46). Activation of EGF signaling in bronchial epithelial repair may augment airway remodeling and contribute to chronic asthma (46).

The increased expression of TGF-β1, TGF-β2, and EGF demonstrates that this model recapitulates the asthmatic growth factor milieu. These findings are evidence for signaling from epithelium to underlying the mesenchyme. It is likely that this signaling is bidirectional (i.e., epithelium to mesenchyme and mesenchyme to epithelium), as recent literature indicates in lung and other organs (47, 48).

We acknowledge that a limitation of our xenograft model is its heterotopic design. Although we provide an airway environment, an orthotopic model, whereby human epithelial cells are grafted onto the *in situ* trachea of a mouse, would provide a more representative environment, including turbulent airflow. However, the damage response of denuding the trachea *in vivo* is a limiting factor toward the development of such an orthotopic model. Despite this limitation, our xenograft model permits cause and effect studies of airway epithelial repair and fibrosis in the lung. To this end, we use the model to provide the first *in vivo* evidence that the asthmatic epithelium alone is sufficient to drive aberrant mesenchymal remodeling. The utility of the xenograft model goes beyond asthma in that there are clear indications for study of airway epithelial cells from individuals with other chronic lung diseases, for instance, chronic obstructive pulmonary disease. Finally, as a single-donor model, the xenografts provide an experimental system to study precision medicine applications, such as individualized drug responses. ■

Author disclosures are available with the text of this article at www.atsjournals.org.

References

1. Lambrecht BN, Hammad H. The airway epithelium in asthma. *Nat Med* 2012;18:684–692.
2. Hallstrand TS, Hackett TL, Altemeier WA, Matute-Bello G, Hansbro PM, Knight DA. Airway epithelial regulation of pulmonary immune homeostasis and inflammation. *Clin Immunol* 2014;151:1–15.
3. Hammad H, Chieppa M, Perros F, Willart MA, Germain RN, Lambrecht BN. House dust mite allergen induces asthma via Toll-like receptor 4 triggering of airway structural cells. *Nat Med* 2009;15:410–416.
4. Holgate ST, Davies DE, Lackie PM, Wilson SJ, Puddicombe SM, Lordan JL. Epithelial–mesenchymal interactions in the pathogenesis of asthma. *J Allergy Clin Immunol* 2000;105:193–204.
5. Hackett TL, de Bruin HG, Shaheen F, van den Berge M, van Oosterhout AJ, Postma DS, Heijink IH. Caveolin-1 controls airway epithelial barrier function: implications for asthma. *Am J Respir Cell Mol Biol* 2013;49: 662–671.
6. Freishtat RJ, Watson AM, Benton AS, Iqbal SF, Pillai DK, Rose MC, Hoffman EP. Asthmatic airway epithelium is intrinsically inflammatory and mitotically dyssynchronous. *Am J Respir Cell Mol Biol* 2011;44: 863–869.
7. Kicic A, Hallstrand TS, Sutanto EN, Stevens PT, Kobor MS, Taplin C, Paré PD, Beyer RP, Stick SM, Knight DA. Decreased fibronectin production significantly contributes to dysregulated repair of asthmatic epithelium. *Am J Respir Crit Care Med* 2010;181:889–898.
8. Broide DH, Lawrence T, Doherty T, Cho JY, Miller M, McElwain K, McElwain S, Karin M. Allergen-induced peribronchial fibrosis and mucus production mediated by IκB kinase β-dependent genes in airway epithelium. *Proc Natl Acad Sci USA* 2005;102:17723–17728.
9. Royce SG, Li X, Tortorella S, Goodings L, Chow BS, Giraud AS, Tang ML, Samuel CS. Mechanistic insights into the contribution of epithelial damage to airway remodeling: novel therapeutic targets for asthma. *Am J Respir Cell Mol Biol* 2014;50:180–192.
10. Reeves SR, Kolstad T, Lien TY, Elliott M, Ziegler SF, Wight TN, Debley JS. Asthmatic airway epithelial cells differentially regulate fibroblast expression of extracellular matrix components. *J Allergy Clin Immunol* 2014;134:663–670.e661.
11. Hackett TL, Warner SM, Stefanowicz D, Shaheen F, Pechkovsky DV, Murray LA, Argentieri R, Kicic A, Stick SM, Bai TR, *et al*. Induction of epithelial–mesenchymal transition in primary airway epithelial cells from patients with asthma by transforming growth factor-β1. *Am J Respir Crit Care Med* 2009;180:122–133.

12. Petersen TH, Calle EA, Zhao L, Lee EJ, Gui L, Raredon MB, Gavrilov K, Yi T, Zhuang ZW, Breuer C, *et al*. Tissue-engineered lungs for *in vivo* implantation. *Science* 2010;329:538–541.
13. Barnes PJ, Bonini S, Seeger W, Belvisi MG, Ward B, Holmes A. Barriers to new drug development in respiratory disease. *Eur Respir J* 2015; 45:1197–1207.
14. Sears MR, Taylor DR. The β2-agonist controversy: observations, explanations and relationship to asthma epidemiology. *Drug Saf* 1994;11:259–283.
15. Filali M, Zhang Y, Ritchie TC, Engelhardt JF. Xenograft model of the CF airway. *Methods Mol Med* 2002;70:537–550.
16. Kipling D, Cooke HJ. Hypervariable ultra-long telomeres in mice. *Nature* 1990;347:400–402.
17. Vander Griend DJ, Konishi Y, De Marzo AM, Isaacs JT, Meeker AK. Dual-label centromere and telomere FISH identifies human, rat, and mouse cell contribution to Multispecies recombinant urogenital sinus xenografts. *Prostate* 2009;69:1557–1564.
18. Davies DE. Epithelial barrier function and immunity in asthma. *Ann Am Thorac Soc* 2014;11:S244–S251.
19. Hackett TL, Singhera GK, Shaheen F, Hayden P, Jackson GR, Hegele RG, Van Eeden S, Bai TR, Dorscheid DR, Knight DA. Intrinsic phenotypic differences of asthmatic epithelium and its inflammatory responses to respiratory syncytial virus and air pollution. *Am J Respir Cell Mol Biol* 2011;45:1090–1100.
20. Richter A, Puddicombe SM, Lordan JL, Bucchieri F, Wilson SJ, Djukanovic R, Dent G, Holgate ST, Davies DE. The contribution of interleukin (IL)-4 and IL-13 to the epithelial–mesenchymal trophic unit in asthma. *Am J Respir Cell Mol Biol* 2001;25:385–391.
21. Derynck R, Zhang YE. Smad-dependent and Smad-independent pathways in TGF-β family signalling. *Nature* 2003;425:577–584.
22. Balzar S, Chu HW, Silkoff P, Cundall M, Trudeau JB, Strand M, Wenzel S. Increased TGF-β2 in severe asthma with eosinophilia. *J Allergy Clin Immunol* 2005;115:110–117.
23. Tamaoka M, Hassan M, McGovern T, Ramos-Barbón D, Jo T, Yoshizawa Y, Tolloczko B, Hamid Q, Martin JG. The epidermal growth factor receptor mediates allergic airway remodelling in the rat. *Eur Respir J* 2008;32:1213–1223.
24. Wang Q, Li H, Yao Y, Xia D, Zhou J.The overexpression of heparin-binding epidermal growth factor is responsible for Th17-induced airway remodeling in an experimental asthma model. *J Immunol* 2010;185:834–841.
25. Butler CR, Hynds RE, Gowers KH, Lee DdoH, Brown JM, Crowley C, Teixeira VH, Smith CM, Urbani L, Hamilton NJ, *et al*. Rapid expansion of human epithelial stem cells suitable for airway tissue engineering. *Am J Respir Crit Care Med* 2016;194:156–168.
26. Davies DE. The role of the epithelium in airway remodeling in asthma. *Proc Am Thorac Soc* 2009;6:678–682.
27. Nawijn MC, Hackett TL, Postma DS, van Oosterhout AJ, Heijink IH. E-cadherin: gatekeeper of airway mucosa and allergic sensitization. *Trends Immunol* 2011;32:248–255.
28. Hayashi T. Molecular mechanisms of metaplasia, differentiation and hyperplasia of goblet cellin allergic asthma. *J Aller Ther* 2012;3:121.
29. Rajavelu P, Chen G, Xu Y, Kitzmiller JA. Airway epithelial SPDEF integrates goblet cell differentiation and pulmonary Th2 inflammation. *J Clin* 2015;125:2021–2031.
30. Cokuğraş H, Akçakaya N, Seçkin, Camcioğlu Y, Sarimurat N, Aksoy F. Ultrastructural examination of bronchial biopsy specimens from children with moderate asthma. *Thorax* 2001;56:25–29.
31. Barbato A, Turato G, Baraldo S, Bazzan E, Calabrese F, Panizzolo C, Zanin ME, Zuin R, Maestrelli P, Fabbri LM, *et al*. Epithelial damage and angiogenesis in the airways of children with asthma. *Am J Respir Crit Care Med* 2006;174:975–981.
32. Fedorov IA, Wilson SJ, Davies DE, Holgate ST. Epithelial stress and structural remodelling in childhood asthma. *Thorax* 2005;60: 389–394.
33. Roth S, Freund I. Second harmonic generation in collagen. *J Chem Phys* 1979;70:1637–1643.
34. Freund I, Deutsch M. Second-harmonic microscopy of biological tissue. *Opt Lett* 1986;11:94.
35. Cicchi R, Vogler N, Kapsokalyvas D, Dietzek B, Popp J, Pavone FS. From molecular structure to tissue architecture: collagen organization probed by SHG microscopy. *J Biophotonics* 2013;6: 129–142.
36. Tschumperlin DJ. Fibroblasts and the ground they walk on. *Physiology* 2013;28:380–390.
37. Van De Water L, Varney S, Tomasek JJ. Mechanoregulation of the myofibroblast in wound contraction, scarring, and fibrosis: opportunities for new therapeutic intervention. *Adv Wound Care (New Rochelle)* 2013;2:122–141.
38. Eckes B, Nischt R, Krieg T. Cell–matrix interactions in dermal repair and scarring. *Fibrogenesis Tissue Repair* 2010;3:4.
39. Seppä H, Grotendorst G, Seppä S, Schiffmann E, Martin GR. Platelet-derived growth factor in chemotactic for fibroblasts. *J Cell Biol* 1982; 92:584–588.
40. Senior RM, Huang JS, Griffin GL, Deuel TF. Dissociation of the chemotactic and mitogenic activities of platelet-derived growth factor by human neutrophil elastase. *J Cell Biol* 1985;100:351–356.
41. Alcala SE, Benton AS, Watson AM, Kureshi S, Reeves EM, Damsker J, Wang Z, Nagaraju K, Anderson J, Williams AM, *et al*. Mitotic asynchrony induces transforming growth factor-β1 secretion from airway epithelium. *Am J Respir Cell Mol Biol* 2014;51:363–369.
42. Oida T, Weiner HL. TGF-β induces surface LAP expression on murine CD4 T cells independent of Foxp3 induction. *PLoS One* 2010;5: e15523.
43. Abnaof K, Mallela N, Walenda G, Meurer SK, Seré K, Lin Q, Smeets B, Hoffmann K, Wagner W, Zenke M, *et al*. TGF-β stimulation in human and murine cells reveals commonly affected biological processes and pathways at transcription level. *BMC Syst Biol* 2014;8:55.
44. Serpero L, Petecchia L, Sabatini F, Giuliani M, Silvestri M, Di Blasi P, Rossi GA. The effect of transforming growth factor (TGF)-β1 and (TGF)-β2 on nasal polyp fibroblast activities involved upper airway remodeling: modulation by fluticasone propionate. *Immunol Lett* 2006;105:61–67.
45. Amishima M, Munakata M, Nasuhara Y, Sato A, Takahashi T, Homma Y, Kawakami Y. Expression of epidermal growth factor and epidermal growth factor receptor immunoreactivity in the asthmatic human airway. *Am J Respir Crit Care Med* 1998;157:1907–1912.
46. Puddicombe SM, Polosa R, Richter A, Krishna MT, Howarth PH, Holgate ST, Davies DE. Involvement of the epidermal growth factor receptor in epithelial repair in asthma. *FASEB J* 2000;14:1362–1374.
47. Wei SC, Fattet L, Tsai JH, Guo Y, Pai VH, Majeski HE, Chen AC, Sah RL, Taylor SS, Engler AJ, *et al*. Matrix stiffness drives epithelial–mesenchymal transition and tumour metastasis through a TWIST1–G3BP2 mechanotransduction pathway. *Nat Cell Biol* 2015; 17:678–688.
48. Volckaert T, Campbell A, Dill E, Li C, Minoo P, De Langhe S. Localized Fgf10 expression is not required for lung branching morphogenesis but prevents differentiation of epithelial progenitors. *Development* 2013;140:3731–3742.